GNSS/IMU Tightly Coupled Scheme with Weighting and FDE for Rail Applications

Xin Han, Syed Ali Kazim, Nourdine Ait Tmazirte, Juliette Marais, Debiao Lu

GNSS/IMU Tightly Coupled Scheme with Weighting and FDE for Rail Applications

Xin Han, *Beijing Jiaotong University, China/COSYS-LEOST, Univ Gustave Eiffel, IFSTTAR, France*
Syed Ali Kazim, *COSYS-LEOST, Univ Gustave Eiffel, IFSTTAR, France*
Nourdine Aït Tmazirte, *Institut de Recherche Technologique Railenium, France*
Juliette Marais, *COSYS-LEOST, Univ Gustave Eiffel, IFSTTAR, France*
Debiao Lu, *Beijing Jiaotong University, China*

BIOGRAPHIES

B. Sc. Xin Han is a graduate student at Beijing Jiaotong University, she received B.Sc. degree in Rail Traffic Signal and Control at Lanzhou Jiaotong University. Her research focuses on performance evaluation of integrated navigation system. She worked within Ifsttar for an internship in the summer 2019.

Dr. Juliette Marais received the engineering degree from Institut Supérieur de l'Electronique et du Numérique. She received the Ph.D. degree in electronics and the "Habilitation à diriger des recherches" from the University of Lille, France, in 2002 and 2017 respectively. Since 2002, she has been a research fellow with IFSTTAR, the French Institute of science and technology for transport, development, and networks. She is involved on two main research projects: integrity monitoring for land transport applications and GNSS propagation characterization in railway environments, with some contributions in EU or national projects. Her research interests principally include propagation phenomena, positioning and pseudorange error modeling, filtering technics, and simulation.

Syed Ali Kazim works as a research engineer at IFSTTAR, the French Institute of science and technology for transport, development, and networks since 2018. His current research interests focus on multipath detection, modelling and mitigation. He is involved in European projects such as ERSAT GGC and Gate4Rail.

Nourdine Aït Tmazirte works at French Institute of Technology Railenium since 2018. He got his engineering and M.Sc. degree in automation engineering from Ecole Centrale de Lille, France, both in 2010. His research interests include multi-sensor fault tolerant fusion for localization and integrity assessment.

Dr.-Ing. Debiao Lu works at faculty of Electronic and Information Engineering at Beijing Jiaotong University in China since 2015. He got his doctor title at faculty of Mechanical Engineering at Technische Universität Braunschweig, Germany in 2014. He received the B.Sc. degree in telecommunication engineering and M.Sc. degree in traffic information engineering and control, both at Beijing Jiaotong University in China. His research interests include GNSS safe localization, GNSS propagation simulation and performance assessment.

ABSTRACT
GNSS used as a standalone positioning system fulfils most of the requirements for many applications since decades. However, the need of high available, accurate and fail-safe positioning systems for new applications such as rail autonomous vehicles for train signaling applications motivates the community to explore novel solutions. In this context, multi-constellation multi-frequency GNSS receivers have the potential to enhance the positioning solutions. However, when applied to safety-critical land transportation system, the localization function not only needs to meet accuracy requirements, but more importantly, it also needs to bound the positioning errors in order to reduce the risk of unexpected and undetected faults.
Thus, in order to reach continuous and fail-safe positioning solutions, the use of complementary heterogeneous sensors with a smart hybridization becomes essential. For safety-related and regulated applications as in railways, one will also need, as a next step, to develop the capacity of assessing the safety of the hybrid solution. The concept of integrity can help to reach this requirement and is currently investigated for rail applications. RAIM (Receiver Autonomous Integrity Monitoring) was first defined for aviation applications and is widely used for their safety assessment. However, due to the different safety requirements and operational environment in aviation and land applications (i.e. railway and road application), dedicated algorithms need to be developed for such

applications. Indeed, terrestrial applications can face particularly harsh environments (urban canyon, forests ...) in which a dilemma appears between the (reduced) availability of visible satellites and the possibility of encountering multiple simultaneous errors (NLOS, multipath interferences ...). Under these conditions, implementing a strategy based solely on a FDE layer can lead to a decrease in the availability of the localization function. Conversely, relying solely on a strategy of weighting observation error models cannot constitute an acceptable solution from a safety point of view. Only a harmonious combination of these two strategies in a stringent environmental condition can achieve the availability and security requirements. With a real dataset collected along a railway line, we compare the positioning accuracy of a GNSS/IMU tightly coupled system before and after weighting and FDE schemes. The results show that the average value of Horizontal Position Error (HPE) has been reduced after applying the performance improvement method on the GNSS/IMU system. It also shows that the implemented Horizontal Protection Level (HPL) correctly bounds HPE.

INTRODUCTION

The worldwide railway community recognizes today GNSS as “a game changer” in future signalling systems. However, it is well known and demonstrated that GNSS are prone to failure in shadowed environments when the train pass through tunnels and bridges for example, which can result in a loss of the positioning function or in urban environments where accuracy will be degraded by signal reception conditions. Therefore, relying on a GNSS-alone navigation system for train positioning cannot meet railway safety requirements.

The inertial navigation system (IMU) is a widely used autonomous navigation system that can work as an independent sensor, without relying on any external information. It offers high precision for short-term and have no influence from the external environment. Integrating GNSS and IMU system can make full use of the advantages of the two subsystems. The GNSS/IMU integrated navigation systems have one of these three structures: loosely coupled, tightly-coupled, and deep-coupled hybridization.

The main advantage of the tightly coupled method is the possibility to update the hybrid navigation solution also in scenarios with a poor signal quality or limited coverage, thanks to the observation vector which is composed of the original pseudorange and pseudorange rate. The tightly coupled method has been widely applied. In order to improve the high-precision navigation and positioning capability of vehicles in harsh environments, [1] uses a low-cost MEMS-IMU and RTK tightly coupled technology to achieve high-precision positioning of vehicles in centimeters. [2] proposes a low-cost SINS/magnetometer (MR) tightly coupled navigation system based on the Kalman filter to increase the accuracy of heading attitude output by MR.

The tightly coupled method makes the performance of the integrated navigation system better than the subsystem through data fusion. We can further improve the performance of the integrated system by improving the performance of the subsystem. In the railway field, the positioning performance of the GNSS/IMU integrated navigation system is crucial. It mainly includes two criteria: accuracy and integrity. Accuracy refers to the proximity between the estimated or measured user position, velocity value and true value. Accuracy is positively correlated with the positioning performance of the system. In the land environment, the positioning performance of the GNSS positioning system is mainly affected by the Non-Line-of-Sight reception and the multipath interference. In [3], a real-time integrated IMU/GPS navigation system for land vehicle applications improves the positioning accuracy by detecting and eliminating abnormal observations caused by the multipath effect. In [4], relying upon a representative analysis of empirical SNR(signal-to-noise-ratio)-based weights, it proposes the elevation dependent exponential weighting function EXPZ, which benefits from realistic SNR-based weights. [5] proposed a novel GNSS measurement error model which combines the information of C/N0 (carrier-power-to-noise-density ratio), satellite elevations, the signal reception state LOS/NLOS as well as the range corrections for NLOS signals to improve positioning performance. The above research aims to estimate accurately the observed noise by establishing a weighting model to improve the positioning accuracy.

Integrity is defined as the measure of the trust that can be placed in the correctness of the information supplied by a navigation system and the ability of the system to provide timely warnings to users when the system should not be used for navigation. Integrity holds the concepts of AL (Alert Limit), IR (Integrity Risk), PL (Protection Level) and TTA (Time To Alert). An integrity monitoring solution uses GNSS signals to detect changes or anomalies in satellite signal characteristics that could affect the accuracy of the position calculated by the user equipment [6]. Therefore, for railway application based on GNSS/IMU, integrity is one of the major indicators for safety. The concept of integrity was formerly targeted at aviation applications. In the aviation, the requirements for integrity monitoring algorithms are relaxed due to the presence of large number of redundant observations. Moreover, it is assumed that one fault is present at maximum in a particular instant. However, in railway applications, due to the influence of NLOS and multipath interference, the above two points are not well satisfied, so the traditional integrity monitoring algorithm cannot be directly applied to the railway. In recent years, there have been some papers studied on the integrity monitoring methods for urban environments. [7] presents a GNSS Aircraft-Based Integrity Augmentation (ABIA) system, which relies on detailed modeling of signal propagation and multipath effects to produce predictive and reactive alerts (cautions and warnings) in urban environments. [8]

proposes a novel concept of "local integrity" suitable to Global Navigation Satellite System (GNSS) receivers in urban vehicular scenarios. The main idea is to take into account not only the system, but also the environment nearby the receiver in its nominal conditions, exploiting the potentialities offered by a Vehicular Ad-hoc Network (VANET) infrastructure. To overcome the urban environment constraints, strongly affecting the positioning performance and to guarantee a satisfying level of trust of the PVT solution. [9] proposes a step-by-step technique consisting of an integrated GPS/Galileo receiver and low-cost MEMS sensors, and aided by a video Fisheye camera and implementing an urban-oriented integrity monitoring technique.
Under the harsh environments of railway application, implementing a strategy based solely on a FDE layer can lead to a decrease in the availability of the localization function. Conversely, relying solely on a strategy of weighting observation error models cannot constitute an acceptable solution from a safety point of view. Therefore, this paper proposed a harmonious combination of these two strategies in a stringent environmental condition to achieve the availability and security requirements.

The paper will be structured as follows: first section defines the principles of the chosen tightly coupled GNSS and IMU positioning system; second one explains how weighting and fault detection allows to enhance its performance; the third describes the computation of the Horizontal Protection Level; last section illustrates performance of these algorithms on a real railway dataset before conclusions and perspectives.

I. EKF-BASED TIGHTLY COUPLED GNSS/IMU POSITIONING SYSTEM

A. GNSS/IMU-based Integrated Navigation System

Merging GNSS and IMU data permits to find a good compromise between a less precise but accurate along time GNSS alone solution and a very precise IMU solution but only in a short-time window. For linear systems, the most commonly used filtering method is Kalman Filter (KF). However, as most of the real systems, as multi-sensor systems, cannot satisfy the assumption of linearity, some extension of KF for non-linear systems are used, as for example, Extended Kalman Filter (EKF), Adaptive Kalman Filter (AKF), Unscented Kalman Filter (UKF) and Particle Filter (PF). Among many nonlinear filtering methods, EFK is widely used due to its simple implementation and easy to integrate with integrity monitoring process. We will use EKF that is based on the assumption that noise is Gaussian distributed. The EKF is based on KF. Its core idea is to perform a first-order Taylor series expansion on the nonlinear function around a predicted value to obtain an approximate linearized model, which is then solved using KF. The essence of KF is a recursive linear variance estimation. The KF consists of a state model and an observation model, as follows:

$$\mathbf{X_k} = \mathbf{\Phi_{k,k-1}} \mathbf{X_{k-1}} + w_{k-1}$$
$$\mathbf{Z_k} = \mathbf{H_k} \mathbf{X_k} + v_k$$

In the state model, X_k is the system state vector, $\Phi_{k/k-1}$ is the state transfer matrix and w_{k-1} denotes the zero-mean Gaussian process model noise.
In the observation model, Z_k is the system observation vector; H_k is the observation matrix and v_k denotes the observation noise.
Around these two models, Kalman Filter estimates the state value through the process described in figure 1. It mainly includes two major parts: time update and measurement update:

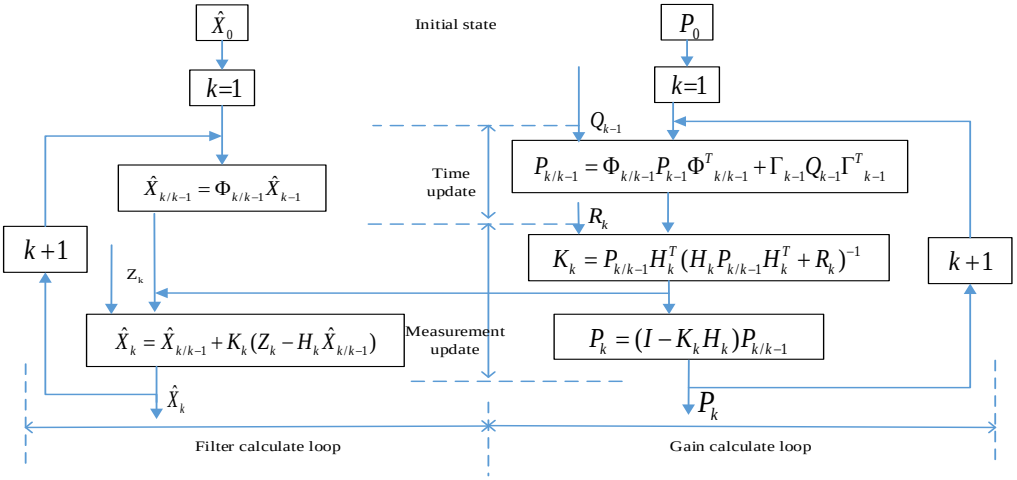

Figure 1. The calculation process of KF.

In figure 1, $P_{k/k-1}$ is the system covariance matrix; K_k is the gain of the Kalman Filter and R_k is the variance of the observation noise. The EKF can realize the integration of GNSS/IMU, making full use of the two technologies advantages to improve train positioning accuracy. Three different integration schemes are possible, namely loosely, tightly and deeply coupling.

In the loosely coupled integration, the difference between the position and speed of both the GNSS and the IMU is used as the input of the Kalman Filter. The loosely coupled system can obtain the 15-dimensional optimal state estimation values, which are the three-dimensional position, velocity, attitude errors of the IMU, and the three-dimensional drift error respectively associated with the accelerometer and gyroscope. Then the accumulated error of the IMU is corrected by the optimal state estimation of the output and obtain a more accurate positioning result. The structure of the loosely coupled is simple and easy to implement, but it needs to be used under the condition that the number of visible satellites is greater than four [3]. Compared with the loosely coupled, the tightly coupled integration directly uses the difference between the original GNSS observations (i.e., pseudorange, pseudorange rate) and the virtual observations derived from the IMU as input to the Kalman Filter. In addition to the estimated 15-dimensional state in the loosely coupled, the tightly coupled system increases the two error estimates associated with the receiver clock, generating a 17-dimensional matrix. On the one hand, the tightly coupled system uses the original observation as the input, eliminating the error of the GNSS positioning process. On the other hand, the algorithm has lower requirements on the number of visible satellites. When the number of visible satellites is less than four, the positioning function can still be achieved [10].

The deeply coupled scheme uses the measurement information of the tracking loop as the input of the Kalman Filter and uses the corrected IMU navigation data to assist the tracking of the GNSS signal. Among the three integrated structures, the deeply coupled has the highest positioning accuracy, but at the same time, its structure is the most complicated and difficult to implement [11].

In this paper, the tightly coupled scheme has been chosen as a compromise between performance and complexity.

B. EKF-based Tightly Coupled GNSS/IMU Positioning System

Figure 2 shows the model of tightly coupled integration inspired by [30]. Here, the EKF is used to estimate the position error $\{\delta p_x, \delta p_y, \delta p_z\}$, and the three components of velocity v, attitude$\emptyset$, accelerometer a and gyro g errors of the IMU as well as the user clock offset δt_u and user clock drift δt_{ru} .

The state vector of the tightly coupled model consists of:

$$\mathbf{X_k} = [\delta\phi_x \;\; \delta\phi_y \;\; \delta\phi_z \;\; \delta v_x \;\; \delta v_y \;\; \delta v_z \;\; \delta p_x \;\; \delta p_y \;\; \delta p_z \;\; \delta a_x \;\; \delta a_y \;\; \delta a_z \;\; \delta g_x \;\; \delta g_y \;\; \delta g_z \;\; \delta t_u \;\; \delta t_{ru} \;\;]^T$$

The observation vector consists of the difference between the two pseudorange and pseudorange rates available, i.e. the ρ and $\dot{\rho}$ estimated from the IMU and provided by the GNSS receiver:

$$\mathbf{Z_k} = \begin{bmatrix} \rho_G - \rho_I \\ \dot{\rho}_G - \dot{\rho}_I \end{bmatrix} = [\delta\rho_1 \;\; \delta\rho_2 \;\; \cdots \;\; \delta\rho_n \;\; \delta\dot{\rho}_1 \;\; \delta\dot{\rho}_2 \;\; \cdots \;\; \delta\dot{\rho}_n]^T$$

Where, n denotes the number of visible satellites and $(\rho_I, \dot{\rho}_I)$ respectively the pseudorange and pseudorange rate estimated from the IMU position estimation.

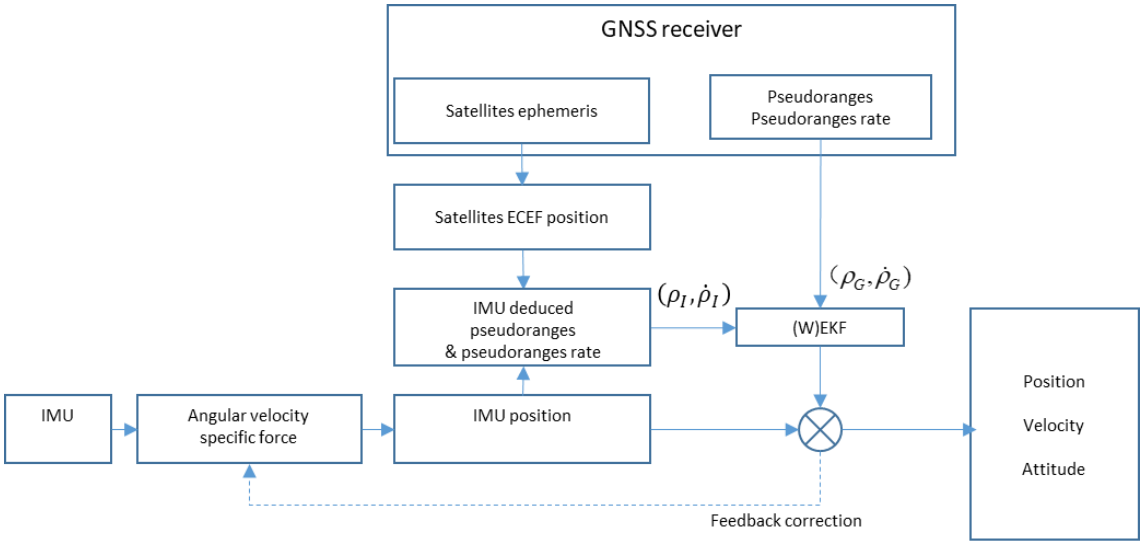

Figure 2. The structure of the tightly coupled system.

The state transition matrix is designed as:

$$\Phi_k = \begin{bmatrix} \Phi_{I,k} & 0 \\ 0 & \Phi_{G,k} \end{bmatrix}$$

Where $\Phi_{I,k}$ is a 15×15 dimensions matrix related to the IMU errors and $\Phi_{G,k}$ is a 2×2 dimensions matrix related to the GNSS errors, specific derivation can refer to [12].

The observation matrix in the EKF is designed as:

$$\mathrm{H}_k = \begin{bmatrix} 0_{n\times 6} & \cup_{n\times 3} & 0_{n\times 6} & 1_{n\times 1} & 0_{n\times 1} \\ 0_{n\times 3} & \cup_{n\times 3} & 0_{n\times 9} & 0_{n\times 1} & 1_{n\times 1} \end{bmatrix}$$

With,

$$\cup_{n\times 3} = \begin{bmatrix} (x^{s_1}-x)/R_{pr}^{s_1} & (y^{s_1}-y)/R_{pr}^{s_1} & (z^{s_1}-z)/R_{pr}^{s_1} \\ \vdots & \vdots & \vdots \\ (x^{s_n}-x)/R_{pr}^{s_n} & (y^{s_n}-y)/R_{pr}^{s_n} & (z^{s_n}-z)/R_{pr}^{s_n} \end{bmatrix}$$

And,

$$R_{pr}^{s_n} = \sqrt{(x^{s_n}-x)^2+(y^{s_n}-y)^2+(z^{s_n}-z)^2}$$

Where, $(x^{s_n}, y^{s_n}, z^{s_n})$ denotes the position of the n^{th} satellite and (x, y, z) the estimated user position both in ECEF coordinates.

According to the Kalman Filter process in Figure 1, using known measurement vector Z_k, the linear optimal estimate of the state can be found.

II. EKF-BASED TIGHTLY COUPLED ALGORITHM

In currently developed tightly coupled integration based on EKF, empirical values are used to estimate the variance of the pseudorange error. A more realistic individual evaluation of pseudorange error could improve the positioning accuracy when the estimated ranging measurement are affected by age of navigation message or the error induced by the local environment. This could increase the pseudorange error, which may result in deviation of the estimated position from the true position. In order to solve the

above problems, a large number of pseudorange error variance estimation methods and fault detection algorithms have been used to improve the traditional EKF algorithm, and it is verified that improvement algorithms have good effects in GNSS alone navigation system [5]. In this article, the performance of the improvement algorithm in a GNSS/IMU tightly coupled system will be discussed.

A. The Weighting Model based on Satellite Elevation

The pseudorange measurement error mainly includes satellite clock error, ionosphere error, tropospheric error, multipath error and receiver clock error. In land applications, a fixed common measurement error variance cannot adapt well to complex environmental changes. The measurement error is also related to the quality of the signal in a particular environment. The most employed criteria to evaluate the signal quality are the Carrier-Power-to-Noise-Density Ratio (C/N0) and the satellite elevation. There are several error variance model presented in the literature as a function of the C/N0, such as the sigma-ε model [13] and the sigma-Δ model [14]. For the satellite elevation, there are several elevation dependent models existing in the literature, such as the model based on sin type [15] and the model based on exponent type [16].

In this paper, we enhanced the classical GNSS/IMU tightly coupled scheme with the easy-to-implement sin type algorithm based on satellite elevation to constructs a weighting model in order to increase accuracy. The weighting model is applied to the tightly coupled algorithm in order to verify the performance compared to a simple equally weighted model.

Theoretically, the local effects generally have less impact on the signal of the satellite at higher elevation, that is to say that satellite elevation is inversely proportional to the pseudorange error variance. So, the sin-type algorithm based on elevation is written as follows [15]:

$$\sigma_i^2 = 1/\sin^2(\theta_i)$$

Where θ_i represents the elevation of the i^{th} satellite;

In the design of the EKF, the covariance matrix of the measurement noise R is diagonal and supposed as time-invariant. Its diagonal components are variances of measurement errors. Therefore, a time-varying weighting model can be established based on the satellite elevation as follows:

$$R = \begin{bmatrix} R_\rho & 0 \\ 0 & R_{\dot\rho} \end{bmatrix} = \begin{bmatrix} \sigma_{\rho 1}^2 & \cdots & \cdots & \cdots & 0 \\ \vdots & \ddots & \vdots & \vdots & \vdots \\ 0 & \cdots & \sigma_{\rho n}^2 & \cdots & 0 \\ 0 & \cdots & \sigma_{\dot\rho 1}^2 & \cdots & 0 \\ \vdots & \vdots & \vdots & \ddots & \vdots \\ 0 & \cdots & \cdots & \cdots & \sigma_{\dot\rho n}^2 \end{bmatrix}$$

Here, R_ρ and R_ρ are respectively the measurement covariance matrix of the pseudorange and pseudorange rate.

B. Innovation-based Classic Test in a Tightly Coupled System

Integrity of the navigation system is defined as a measure of trust that can be placed in the correctness of the information supplied by the total system [17]. Integrity monitoring algorithms developed for land vehicles are mostly based on the principles of the traditional Receiver Autonomous Integrity Monitoring (RAIM). RAIM may include the function of fault detection and exclusion (FDE). The essence of the FDE algorithm is to eliminate abnormal measurements by performing consistency checks on measurement residuals. Therefore, FDE can contribute to improving the positioning accuracy as well as the weighting process.

At present, the EKF-based integrity monitoring approach has attracted more and more attention [18-21, 29]. In [5], the EKF Innovation-based Classic Test and the EKF Innovation-based Danish (IBDAN) methods are proposed and verified in the GNSS alone configuration. Among them, the IBCT method is simple to implement, and can directly use the parameters in the tightly coupled model to complete the integrity monitoring, so this paper will analyze the performance of the IBCT method in the GNSS/IMU integrated navigation system.

The IBCT method uses the innovation of EKF to realize fault detection and exclusion. The innovation of EKF at time k can be written as:

$$\gamma_k = z_k - \mathrm{H}_\mathrm{k}\hat{x}_k^-$$

Where, z_k is the real measurement and $\mathrm{H_k}\hat{x}_k^-$ is the predicted measurement.

The covariance matrix S of the innovation vector can be derived as:

$$\mathrm{S_k = H_k P_k^- H_k^T + R_k}$$

Firstly, the fault detection is carried out with a Global Test, and the following assumptions are made: if the system has no fault, the innovation follows the central chi-square distribution; otherwise, the innovation follows the non-central chi-square distribution. The probability density function of the chi-square distribution is:

$$f(x;k) = \begin{cases} \dfrac{x^{\frac{k}{2}-1} e^{-\frac{x}{2}}}{2^{\frac{k}{2}} \Gamma(\frac{k}{2})}, x > 0 \\ 0 \qquad\qquad , otherwise \end{cases}$$

Where, Γ is a function of *k*:

$$\Gamma(\frac{k}{2}) = \int_0^\infty x^{\frac{k}{2}-1} e^{-x} dx$$

According to the chi-square distribution function, with a given P_{fa}, the detection threshold T_k is obtained:

$$P_{fa} = \int_{T_k}^\infty f(x;n_k)dx = \int_{T_k}^\infty \frac{1}{2^{\frac{n_k}{2}} \Gamma(\frac{n_k}{2})} x^{\frac{n_k}{2}-1} e^{-\frac{x}{2}} dx$$

Where P_{fa} denotes the probability of false alarm and n_k denotes the number of visible satellites.

Calculating detection statistics by the Normalized Innovation Squared (NIS):

$$q_k = \gamma_k^T S_k^{-1} \gamma_k$$

Comparing the detection statistic with the detection threshold, if $q_k > T_k$, it indicates that there exists one or several fault(s).

In a second step, the fault exclusion procedure will start in order to isolate the faulty measurements. The essence of fault exclusion is to detect faults for all measurement. If a fault is detected, the corresponding measurement should be excluded.

The innovations cannot be normalized simply by dividing the corresponding diagonal term of its covariance matrix S, due to the matrix S involves the cross correlations of the state components. [22] proposes to use the Cholesky decomposition to remove correlations. It can be written as:

$$\mathrm{S^{-1} = M^T M}$$

Where, the matrix *M* is a lower triangular.

Then, use the matrix *M* to normalize the innovation and identify the fault by the normalized innovation:

$$\tilde{\gamma} = \mathrm{M}\gamma$$

When a fault is detected by the initial Global Test, the biggest normalized innovation $\tilde{\gamma}_i$ is selected in order to exclude the corresponding measurement. The *NIS* is then computed after exclusion and the procedure can be repeated until the test do not fail anymore ($q_k < T_k$) or the number of measurements becomes too small and the solution is declared unreliable.

III. EKF-BASED HPL ALGORITHM

The aim of integrity monitoring is to provide timely warnings to users when the system results are abnormal or unavailable for navigation. Therefore, when using GNSS for safe positioning, the layer of integrity monitoring becomes necessary. Integrity monitoring involves the following important parameters: Alert Limit (AL), Protection Level (PL) and Position Error (PE). By analyzing the relationship between these three parameters, the current state of the system can be given. The relationship between the integrity parameters and the system state has been clearly analyzed in the literature [5]. In safety critical applications, it is necessary and mandatory to meet PL>PE and to ensure that the probability of PE not properly bounded is below a certain limit. The AL is defined by a user according to its application requirements. The PE can be obtained when a ground truth is known, by computing the difference between the true position and the estimated position of the navigation system. Therefore, AL and PE are fixed at a specific

time, but different PL computations can be found in the literature. The objective is to select the most appropriate computation that will properly bound the estimated PE, ideally just bigger than PE but not too much.

The PL is a statistical error bound, which characterizes the maximum allowed positioning error. It can be composed of the Horizontal Protection Level (HPL) and the Vertical Protection Level (VPL). For a railway application, we focus on the horizontal dimension only. The calculation of HPL consists of two parts: the HPL_b under the influence of fault deviation and the HPL_n under the influence of noise. The HPL is the sum of the two as follows [23]:

$$HPL = HPL_b + HPL_n$$

Each part of the equation can be expressed as:

$$HPL_b = \max(Hslope_i) \times pbias$$
$$HPL_n = K(P_{md})d_{major}$$

Where the $Hslope$ represents the satellite feature slope and the $\max(Hslope_i)$ represents the worst-case satellite feature slope.

The $pbias$ denotes the bias in the domain of test statistic. Different values of $pbias$ can be found in the literature depending on the degree of conservatism the user want to apply [24][25]; Here: $pbias = \sigma_i\sqrt{\lambda_k}$ with σ_i denotes the standard deviation of the *ith* measurement error and λ_k denotes the non-centrality parameter;

$K(P_{md})$ is an inflation factor applied to meet the specified integrity risk;

d_{major} is the position error uncertainty along the semi-major axis of the error ellipse, it can be written as: $d_{major} = \sqrt{P_{ee} + P_{nn}}$ where, P_{ee} and P_{nn} are the elements of the estimated state variance matrix P , respectively representing the position variances in the east and north directions.

The relationship between $Hslope$ and HPL_b is illustrated in figure 3 [26]. As expressed in [5][27], the term $Hslope$ represents the sensitivity of HPE to the bias of the i^{th} satellite. For a given HPE, the satellite with the largest $Hslope$ is the most difficult satellite to detect because it corresponds to the smallest detection test statistic. As a result, the probability of missed detection will be the largest. Therefore, when the satellite with the largest $Hslope$ can satisfies the given missed detection rate, its corresponding HPE will be the largest and can be considered as HPL_b .

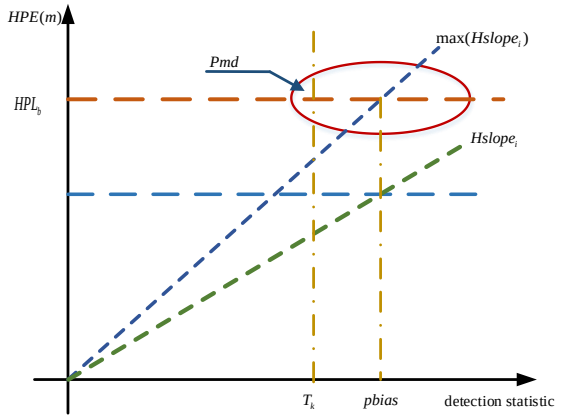

Figure 3 .The relationship between HPL_b and $Hslope$.

As can be seen from figure 3, $Hslope$ is the ratio of the HPE to the detection statistic, which can be calculated by the following formula:

$$Hslope = \sqrt{\frac{E[\varepsilon_e]^2 + E[\varepsilon_n]^2}{E[\gamma_k^T]S_k^{-1}E[\gamma_k]}}$$

Where, ε_e and ε_n are respectively the error between state vector estimation and the true value in the east and north directions. γ_k is the EKF innovation and S_k is the covariance matrix introduced in the section II.
According to the derivation in the literature [5]:

$$E[\varepsilon_k] = K_k^{'}\Phi E[\varepsilon_{k-1}] + K_k E[v_k]$$
$$E[\gamma_k] = -H_k\Phi E[\varepsilon_{k-1}] + H_k E[w_{k-1}] + E[v_k]$$

Therefore, if there is no fault at the last time, the calculation formula of $Hslope$ is as follows:

$$Hslope_i = \sqrt{\frac{f_i^T K_k^T \tau_e^T \tau_e K_k f_i + f_i^T K_k^T \tau_n^T \tau_n K_k f_i}{f_i^T S_k^{-1} f_i}}$$

Where, f_i is a fault profile vector containing zeros except for the corresponding satellite under evaluation, K_k is the EKF gain, τ_e and τ_n are the vector to respectively select the east position state and the north position state form the full state vector.
If there exists a fault at the last epoch, $Hslope$ can be calculated by the following formula [29]:

$$Hslope_i = \sqrt{\frac{f_{(k-1/k),i}^T A_k^T \tau_e^T \tau_e A_k f_{(k-1/k),i} + f_{(k-1/k),i}^T A_k^T \tau_n^T \tau_n A_k f_{(k-1/k),i}}{f_{(k-1/k),i}^T B_k^T S_k^{-1} B_k f_{(k/k-1),i}}}$$

In here,

$$f_{(k-1/k),i} = [\, f_{k-1} \;\; f_k \,]^T,\; A_k = [K_k^{'}\Phi K_{k-1} \;\; K_k],\; B_k = [-H_k\Phi K_{k-1} \;\; I]$$

[5] has verified that the algorithm had good performance in the GNSS-alone navigation system. In this paper, firstly, we use the previous FDE algorithm to detect whether there is a fault at the last epoch. Then, according to the detection result, the corresponding Hslope algorithm is chosen to calculate HPL of the GNSS/IMU tightly coupled system.

IV. APPLICATION

In the last section of the paper, the algorithms described in the first sections of this paper will be evaluated, using a dataset acquired along a railway line.

A. Data used

The objective of the data used in this paper is to illustrate the method expressed in the firsts sections. The algorithms are thus applied here on a dataset representative of an open sky environment along the track, that are the optimal signal reception conditions.
The data have been acquired with a SPAN iMAR FSAS NovAtel system. The length of the data is 1156 epochs approximately 50km long. In absence of another independent reference system, for the reference track, we use the hybridized output of the system, considered as the best trajectory available along this track. They are extracted from the INSPVASA output given by the system. The raw data used as input of our filter algorithm are extracted from the .gps file converted into RINEX file containing satellite positions and pseudoranges.
In the following part, the HPE will represent the distance between the estimated point and the solution of the reference system. Due to a post calibration of the IMU and antenna distance, we will consider this HPE as an “estimated error” more than a “true error” to keep in mind some uncertainty. For further performance assessment, a robust ground truth will be required.

B. Performance analysis

Performances will be compared in terms of accuracy and integrity in order to highlight the benefit of the hybridization and in particular of the enhanced algorithm proposed in this paper.
For the traditional GNSS/INS tightly coupled integrated algorithm, the measurement covariance matrix uses empirical values. Its diagonal components are variances of measurement errors. This paper establishes a weighting matrix based on the satellite elevation to estimate dynamically the measurement matrix R. Following figures show a comparison of the results with and without weighting method.

Figure 4 shows the accuracy enhancement provided by the weighting scheme. The figure shows that most of the time, the elevation-based weighting scheme enhances accuracy by given a higher weight to the highest satellites above the horizon. The particular case of the HPE increase that is visible after epoch 500 illustrates that the chosen weighting scheme can be discussed. The elevation-based weight increases the contribution of a high-elevation satellite without any a priori knowledge about its health or quality and this satellite can decrease accuracy in case of fault. This is a limit of using elevation (alone) based weighting. To mitigate such events, some other weighting schemes can be investigated as some are described in [5].

A bias is observed on the EKF error curve. This bias is relatively slow considering the distance performed by the train (2m error for 50km travelled) and we can see that the bias is decreased after weighting. However, we expect that a finest tuning of the filter will better balance the use of IMU compared to GNSS in order to mitigate such errors.

Whatever the filter used, figures 5 and 6 show that the HPL proposed correctly bounds the HPE. Moreover, the figures show that the weighting schemes allows reducing the size of the HPL. This reduction is important for users as it will increase the usability of the position. Thanks to the weighting scheme proposed, along this line, an alert limit of 10 meters could be accepted. Such a decrease of the HPL allow to increase the capacity of the railway line by simple weighting scheme.

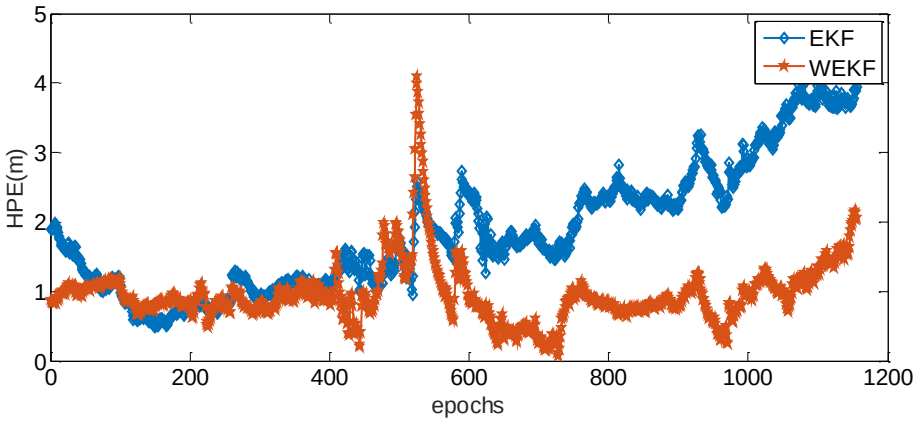

Figure 4. Comparison of HPE after EKF without and with the weighting stage.

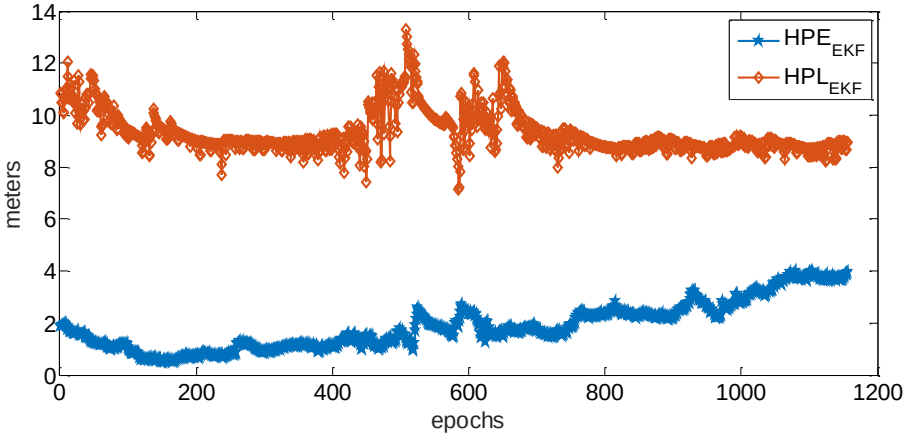

Figure 5. HPE and HPL computed with EKF only.

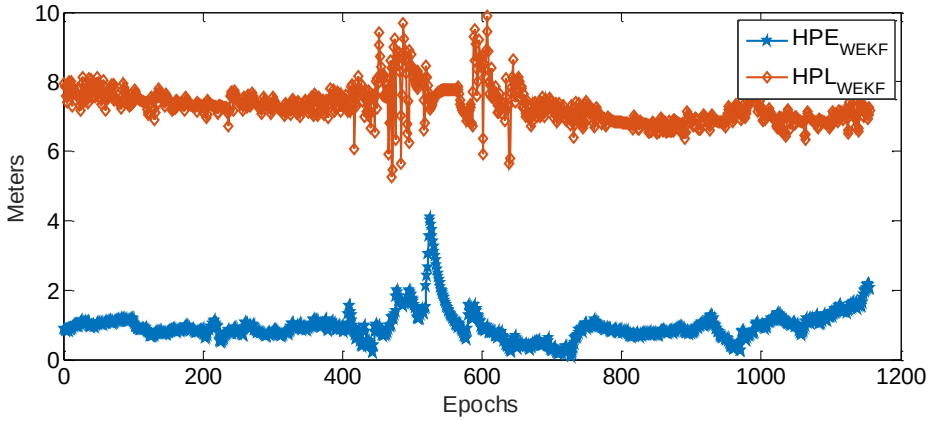

Figure 6. HPE and HPL computed with the WEKF.

Figure 7 shows these conclusions as a Stanford plot. For this figure, the Alert Limit is set to 20m that is a value discussed in some European groups for ERTMS applications. This plot highlights the bounding efficiency of the proposed algorithm as well as the reduction of the maximum error thanks to the weighting proposed. With the weighting scheme, the AL could be lowered for operation efficiency.

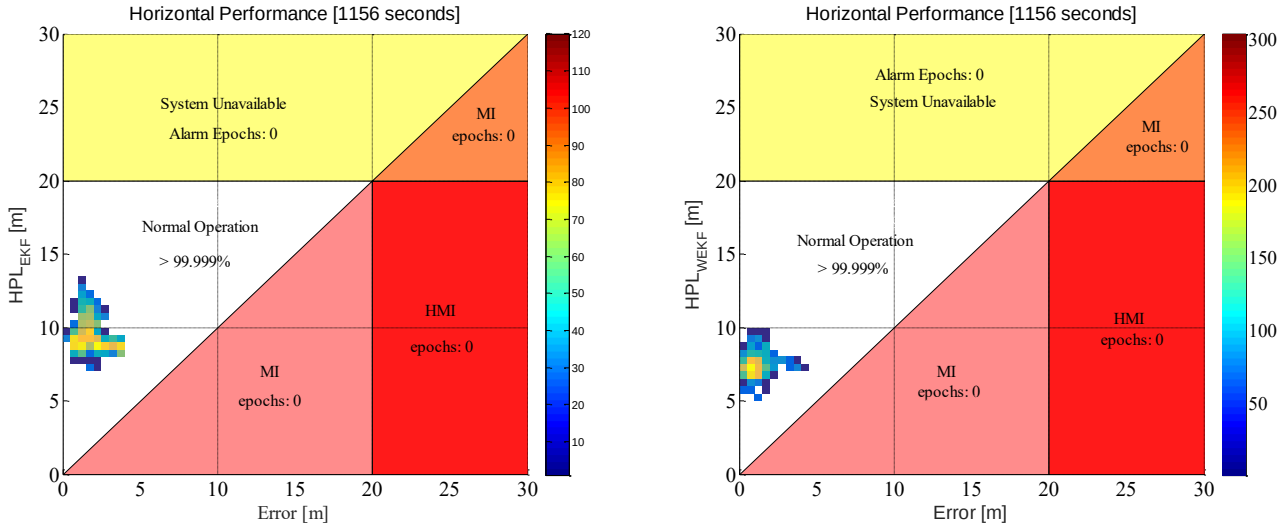

Figure 7. Stanford plots of performance obtained with EKF (left) and WEKF (right).

For the results without weighting, the average horizontal positioning error is 1.87 meters and the average horizontal protection level is 9.30 meters. For the results with weighting, the average horizontal positioning error is 0.96 meters and the average horizontal protection level is 6.35 meters.

Then based on the WEKF algorithm, the performance of the fault detection and exclusion method is evaluated. The essence of the FDE is to eliminate abnormal measurements by performing consistency checks on measurement residuals. Therefore, FDE can contribute to improving the positioning accuracy as well as the weighting process.

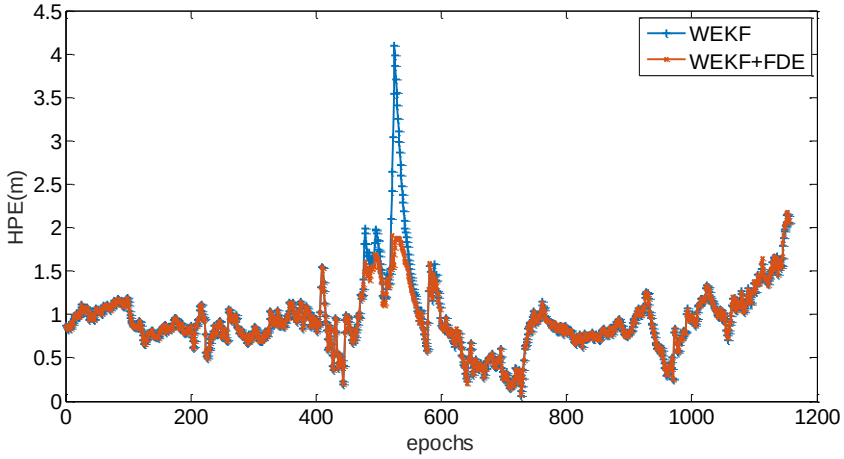

Figure 7. Impact of FDE on the WEKF HPE.

The discussion on figure 4 showed an unexpected increase of HPE around epoch 500. Fortunately, the FDE stage can detect and exclude such an error by detecting the faulty satellite as shown on figure 8.

As can be seen from the figures and table 1, the FDE algorithm impacts the highest values of HPE. The benefit in terms of accuracy is relatively low in this really good environment of reception and with the highly accurate equipment used. It can reduce the mean positioning error from 0.96 meters to 0.93 meters and the standard deviation of the error from 0.44 meters to 0.34 meters. The results also show that the FDE enhances the robustness of the system. In order to reduce the risk that HPL cannot be bound to HPE because of the assumption that there is no prior fault, this paper uses an HPL estimation method combining the results of prior fault detection. Therefore, as shown in table 1, the FDE method leads the HPL increases significantly at several fault epochs.

Table 1. Performances Analysis for the weighting and FDE algorithms.

Estimator type	HPE(m)				HPL_innovation(m)			
	50%	mean	95%	std	50%	mean	95%	std
EKF	1.67	1.87	3.75	0.91	9.00	9.30	11.11	0.81
WEKF without FDE	0.89	0.96	1.66	0.44	6.32	6.35	6.82	0.42
WEKF with FDE	0.89	0.93	1.57	0.34	6.32	6.59	6.84	2.82

CONCLUSIONS AND PERSPECTIVES

To provide a fail-safe accurate positioning solution for railway safety application based on GNSS signals remains a challenge due to the local effects caused by the railway environment on the signal reception. For the automotive applications, some multi-sensor hybridization schemes are already largely investigated but in the railway applications, operational constraints, such as equipment installation but also costs or maintenance needs, have to be taken into account in order to answer this critical issue with feasible and acceptable solutions. In this paper, we have proposed a first scheme, composed of a COTS GNSS and an IMU. The application of this scheme on a first real dataset has shown its capacity to enhance accuracy but ensuring a correct bounding by the proposed HPL. Considering the results presented in this paper, some perspectives can be: First, the choice of the weighting scheme can be enhanced. As shown on figure 4, the elevation as single criterion can mislead the system. Some weighting taking into account more information such as the state of reception [15] or the DOP [27] can be explored and compared.
The RAIM algorithm applied in this paper is GNSS-centered. However, one can discuss the possibility to bound the INS error also as introduced in [28]. From a safety perspective, it is important to evaluate how the system can continue to provide a safe position even in failure or absence of GNSS signals and not focus the entire RAIM scheme on GNSS availability.
As discussed before, the benefit of our proposal applied on this dataset did not show its full potential. Indeed, in a more constrained environment, the effect of FDE will be more visible as seen in [5] in road urban applications. In the future work and in future projects,

the presented solution will have to be evaluated and assessed on different types of tracks in order to check its robustness to rail faulty events, in particular in more constrained areas where we will face different events.
Different types of components (GNSS receiver and IMU) with different costs and performances should also be tested in order to evaluate the impact of each of them on the performance reached.
In the European context, today, these efforts are important in order to offer to the railway users and signaling suppliers some contributions for evaluating reachable performances. Furthermore, such contributions may be useful to help defining architecture of final systems.

ACKNOWLEDGMENTS

The authors acknowledge the support of the Beijing Science Program of Beijing Municipal Science and Technology (No.Z181100001018032) as well as the support of the ELSAT2020 project. The ELSAT2020 project is co-financed by the European Union with the European Regional Development Fund, the French state and the Hauts de France Region Council.

REFERENCES

1. S. Zhu, S. H. Li and Y. Liu, “Low-Cost MEMS-IMU/RTK Tightly Coupled Vehicle Navigation System with Robust Lane-Level Position Accuracy,” *2019 26th Saint Petersburg International Conference on Integrated Navigation Systems (ICINS)*, 2019, pp. 1-4.
2. X. Zhou, D. Chao and L. Song, “Study on the low-cost SINS/MR tightly-coupled navigation technique,” *2013 IEEE International Conference of IEEE Region 10 (TENCON 2013)*, 2013, pp. 1-4.
3. M. L. Cherif, J. Leclère and R. J. Landry, “Loosely coupled GPS/INS integration with snap to road for low-cost land vehicle navigation: EKF-STR for low-cost applications,” *2018 IEEE/ION Position, Location and Navigation Symposium (PLANS)*, 2018, pp. 275-282.
4. X. Luo, M. Mayer, B. Heck and J. L. Awange, "A Realistic and Easy-to-Implement Weighting Model for GPS Phase Observations," *in IEEE Transactions on Geoscience and Remote Sensing*, vol. 52, no. 10, 2014, pp. 6110-6118.
5. Zhu, Ni, “GNSS Propagation Channel Modeling in Constrained Environments: Contribution to the Improvement of the Geolocation Service Quality,” *Université Lille*, 2018.
6. Ni Zhu, Juliette Marais, David Bétaille, Marion Berbineau, "Integrity in Urban Environment: A Review of Literature," *IEEE Transactions on ITS* 19(9): 2762-2778 (2018),
7. S. Bijjahalli, S. Ramasamy and R. Sabatini, "Masking and multipath analysis for unmanned aerial vehicles in an urban environment," *2016 IEEE/AIAA 35th Digital Avionics Systems Conference (DASC)*, 2016, pp. 1-9.
8. D. Margaria and E. Falletti, "A novel local integrity concept for GNSS receivers in urban vehicular contexts," *2014 IEEE/ION Position, Location and Navigation Symposium-PLANS 2014*, 2014, pp. 413-425.
9. E. Shytermeja, A. Garcia-Pena and O. Julien, "Proposed architecture for integrity monitoring of a GNSS/MEMS system with a Fisheye camera in urban environment," *International Conference on Localization and GNSS 2014 (ICL-GNSS 2014)*, 2014, pp. 1-6.
10. G. Falco, M. Pini, and G. Marucco, “Loose and tight GNSS/INS integrations: Comparison of performance assessed in real urban scenarios,” *Sensors*, vol. 17, no. 2, 2017.
11. M. Kirkko-Jaakkola, L. Ruotsalainen and M. Z. H. Bhuiyan, “Performance of a MEMS IMU deeply coupled with a GNSS receiver under jamming,” *2014 Ubiquitous Positioning Indoor Navigation and Location Based Service (UPINLBS)*, 2014, pp. 64-70.
12. Jing-Song Li, “Research on Integrated Navigation Technology Based on Pseudorange and Pseudorange Rate,” *Nanjing University of Science and Technology*, 2009.
13. H. Hartinger and F. Brunner, “Variances of gps phase observations: the sigma-ε model,” *GPS solutions*, vol. 2, no. 4, 1999, pp. 35–43.
14. F. Brunner, H. Hartinger, and L. Troyer, “Gps signal diffraction modelling: the stochastic sigma-δ model,” *Journal of Geodesy*, vol. 73, no. 5, 1999, pp. 259–267.

15. S. Tay and J. Marais, “Weighting models for GPS pseudorange observations for land transportation in urban canyons,” *in 6th European Workshop on GNSS Signals and Signal Processing*, 2013.
16. B. Li, L. Lou, and Y. Shen, “Gnss elevation-dependent stochastic modeling and its impacts on the statistic testing,” *Journal of Surveying Engineering*, vol. 142, no. 2, 2015.
17. M. Jonáš, “GNSS Integrity for Railway Transportation,” *Transactions on Transport Sciences*, vol.4, no. 4, 2011, pp. 183-192.
18. U. I. Bhatti and W. Y. Ochieng, “Detecting multiple failures in gps/ins integrated system: a novel architecture for integrity monitoring,” *Journal of Global Positioning Systems*, vol. 8, no. 1, 2009, pp. 26–42.
19. C. Call, M. Ibis, J. McDonald, and K. Vanderwerf, “Performance of honeywell’s inertial/gps hybrid (high) for rnp operations,” *in Position, Location, And Navigation Symposium (ION PLANS 2006)*, 2006, p. 244.
20. Ç. Tanıl, S. Khanafseh, M. Joerger, and B. Pervan, “Kalman filter-based INS monitor to detect GNSS spoofers capable of tracking aircraft position,” *in Position, Location and Navigation Symposium (ION PLANS 2016)*, 2016, pp. 1027–1034.
21. M. Joerger and B. Pervan, “Kalman filter-based integrity monitoring against sensor faults,” *Journal of Guidance, Control, and Dynamics*, vol. 36, no. 2, 2013, pp. 349–361.
22. O. Le Marchand, “Autonomous approach for localization and integrity monitoring of aground vehicle in complex environment,” *Theses, Université de Technologie de Compiègne*, June, 2010.
23. N. Zhu, D. Bétaille, J. Marais, M. Berbineau, “GNSS Integrity Enhancement for urban Transport Applications by Error Characterization and Fault Detection and Exclusion (FDE)”, *Journées scientifiques 2018 d'URSI-France*, 28-29 mars 2018, Meudon.
24. Tong Haibo, Zhang Guozhu, Ou, Gang, “GNSS RAIM Availability Assessment for Worldwide Precision Approaches,” *2011 International Workshop on Multi-Platform/Multi-Sensor Remote Sensing and Mapping*, 2011, pp. 1-4.
25. S. Bhattacharyya and D. Gebre-Egziabher, “Kalman filter–based RAIM for GNSS receivers,” i*n IEEE Transactions on Aerospace and Electronic Systems*, vol. 51, no. 3, pp. 2444-2459, 2015.
26. Xian-Li Su, “The Research on GNSS Integrity Monitoring Theory and Assisted Performance Enhancement Technique [D],” *Shanghai Jiao Tong University*, 2013.
27. A. Grosch, O. García Crespillo, I. Martini and C. Günther, "Snapshot residual and Kalman Filter based fault detection and exclusion schemes for robust railway navigation," *2017 European Navigation Conference (ENC)*, Lausanne, 2017, pp. 36-47.
28. C. Legrand, J. Beugin, B. Conrard, J. Marais, M. Berbineau, E.-M. El-Koursi, From extended integrity monitoring to the safety evaluation of satellite-based localisation system, *Reliability Engineering & System Safety*, Volume 155, November 2016, Pages 105–114.
29. Crespillo, O. G., Grosch, A., Skaloud, J., & Meurer, M. (2017, September). Innovation vs residual kf based gnss/ins autonomous integrity monitoring in single fault scenario. In Proceedings of the 30th International Technical Meeting of The Satellite Division of the Institute of Navigation (ION GNSS+ 2017), Portland, Oregon (pp. 2126-2136).
30. Groves, P. D. (2013). Principles of GNSS, inertial, and multisensor integrated navigation systems. Artech house.